Received: 28 February 2022 | Revised: 14 July 2022 | Accepted: 25 July 2022

DOI: 10.1002/cem.3438

SPECIAL ISSUE - RESEARCH ARTICLE

Journal of CHEMOMETRICS WILEY

Application of chemometrics on Raman spectra from Mars: Recent advances and future perspectives

Marco Veneranda[1] | **Jose Antonio Manrique**[1] | **Aurelio Sanz-Arranz**[1] | **Sofia Julve Gonzalez**[1] | **Clara Prieto Garcia**[1] | **Elena Pascual Sanchez**[1] | **Menelaos Konstantinidis**[2] | **Elena Charro**[1] | **Jose Manuel Lopez**[1] | **Manuel Angel Gonzalez**[1] | **Fernando Rull**[1] | **Guillermo Lopez-Reyes**[1]

[1]University of Valladolid, Valladolid, Spain

[2]York University, Toronto, Ontario, Canada

Correspondence
Marco Veneranda, University of Valladolid, Spain. Ave. Francisco Vallés. 8. Boecillo 47151, Spain.
Email: marco.veneranda.87@gmail.com

Funding information
Ministry of Economy and Competitiveness, Grant/Award Number: PID2019-107442RBC31; European Union's Horizon 2020 Research and Innovation Programme, Grant/Award Number: 687302

Abstract

The SuperCam and SHERLOC instruments onboard the NASA/Perseverance rover are returning the first Raman spectra to be ever collected from another planet. Similarly, the RLS instrument onboard the ESA/Rosalind Franklin rover will collect Raman spectra from powdered rocks sampled from the subsurface of Mars. To optimize the scientific exploitation of Raman spectra returned from planetary exploration missions, tailored chemometric tools are being developed that take into account the analytical capability of the mentioned Raman spectrometers. In this framework, the ERICA research group is using laboratory simulators of SuperCam and RLS to perform representative laboratory studies that will enhance the scientific outcome of both Mars2020 and ExoMars missions. On one hand, preliminary studies proved the chemometric analysis of RLS datasets could be used to obtain a reliable semi-quantitative estimation of the main mineral phases composing Martian geological samples. On the other hand, it was proved the data fusion of Raman and LIBS spectra gathered by SuperCam could be used to enhance the discrimination of mineral phases from remote geological targets. Besides describing the models developed by the ERICA group, this work presents an overview of the complementary chemometric approaches so far tested in this field of study and propose further improvements to be addressed in the future.

KEYWORDS

chemometrics, ExoMars, Mars, Mars2020, Raman

1 | INTRODUCTION

Most of the scientific discoveries achieved by exploration rovers on Mars have been driven by the use of spectroscopic instruments. Starting from the Sojourner rover (Pathfinder mission) landed on the Ares Vallis region in 1997, the Alpha Particle X-ray Spectrometer (APXS) onboard the vehicle successfully investigated the chemical composition of Martian rocks and regolith over a period of 96 sols.[1] Carrying identical sets of science instruments, Spirit[2] and Opportunity[3] rovers (Mars Exploration Rover missions, MER) landed on Mars in 2004 successfully conducted geological investigations of the Martian surface by combining elemental APXS data[4] with the mineralogical information gathered by Mössbauer[5,6] and Miniature Thermal Emission Spectrometer (Mini-TES)[7] systems. Deepening the current understanding about the geological composition and evolution of Mars, the analytical payload of the Curiosity rover[8] (Mars Science Laboratory mission, MLS) landed on Gale crater in 2012 and still operating includes three spectrometers: an APXS,[9] an X-Ray fluorescence instrument (XRF, as part of the CheMin instrument[10]) and a Laser Induced Breakdown Spectrometer (LIBS system, known as ChemCam[11]).

The set of spectroscopic data gathered over the past three decades allowed the achievement of unprecedented scientific discoveries. Besides reconstructing the geological composition and evolution of Mars,[6,12] the discovery of surficial water-related alteration features proved that Mars had habitable conditions in the past.[13] These findings have paved the way for a new generation of exploration missions, the objective of which is to search for evidence of ancient or present life on Mars.[14,15] To fulfill this objective, the scientific strategy established for current and forthcoming rover missions strongly relies on the use of the first Raman spectrometers to be ever operated beyond terrestrial boundaries. For instance, the analytical payload of the Mars 2020/Perseverance rover[15] (landed on Jezero Crater in 2021) allows to perform both proximity and remote Raman investigations. On one hand, the molecular investigation of proximity targets is performed by SHERLOC,[16] a UV Raman spectrometer whose design has been optimized for the detection of organics. On the other hand, the remote spectroscopic investigation of remote targets is entrusted to SuperCam,[17–19] a multi-analytical suite capable of combining time-resolved Raman analysis with complementary LIBS, VISIR, and luminescence investigations. Besides SHERLOC and SuperCam, a third Raman spectrometer will be deployed on Mars: as part of the ExoMars analytical payload, the Raman Laser Spectrometer (RLS[20]) onboard the Rosalind Franklin rover will perform multiple analyses on powdered subsurface samples (together with complementary MicrOmega NIR data[21]) to select the optimal geological targets to be characterized by the Mars Organic Molecule Analyzer (MOMA) system.[22] Beyond Mars, Raman spectrometers will be employed to explore further celestial bodies, including Phobos (the RAX Instrument[23] for the Martian Moons eXploration mission MMX[24] coordinated by JAXA is currently under development) and Europa (Raman spectroscopy has been selected among the techniques necessary to meet the science goals outlined for the Europa Lander mission[25–27]).

Having clear in mind the critical role Raman spectroscopy will play in planetary exploration missions, it is imperative to develop tailored tools that, taking into consideration the analytical performances and nominal operational modes of the flight instruments, could help maximizing their scientific return. Learning from terrestrial applications, the information extrapolated from Raman spectra can be optimized by the use of chemometric strategies. In recent years, the chemometric analysis of Raman datasets has found a fruitful application in many disciplines, including forensic science,[28,29] environmental pollution,[30,31] conservation science,[32,33] food chemistry,[34,35] pharmaceutic,[36,37] and medical science.[35,38] As a result, chemometric analysis in conjunction with Raman spectroscopy proved to be a reliable approach for spectra calibration,[39,40] identification,[41,42] classification,[43,44] and quantification[45,46] purposes. The advantages of employing chemometric strategies are particularly evident when Raman spectra need to be evaluated in combination with complementary data sets. Focusing on spectroscopic techniques, several works highlight the chemometric analysis of combined complementary data (e.g., Raman-FTIR,[47,48] Raman-LIBS,[49,50] and Raman-XRF[51,52]) provides more detailed information about the investigated target over mono-analytical interpretations strategies.

Unlike terrestrial applications, the development of tailored chemometric strategies to optimize the scientific return of Raman spectra from Mars is still in its initial stage. Indeed, as the development of flight spares models and representative laboratory prototypes is extremely recent, the science teams of ExoMars and Mars 2020 missions have just acquired the necessary analytical tools to reliably simulate Raman datasets from Mars.[53,54] As a result, the great majority of the scientific articles addressing the development/application of chemometric tools to Martian relevant/simulated data have been published in the last few years.[55–58]

Being directly involved in the design and development of SuperCam and RLS systems, the ERICA research group (University of Valladolid, Spain) contributes to this upcoming field of study. As the main advantage of the SuperCam instrument is the capability to perform complementary spectroscopic analysis at the same spot of interest,[17] the ERICA

group is investigating low- and mid-level data fusion approaches to optimize the analytical discrimination of mineral phases. Furthermore as the RLS will investigate between 20 and 39 spots of interest from each Martian sample,[20] representative datasets are being used to develop tailored mineral semi-quantification and rock classification strategies.

Aiming to describe the recent progress made in both research lines, the present manuscript presents the chemometric tools the ERICA research group is developing in the framework of ExoMars and Mars 2020 missions. After describing the application of the preliminary models to Martian-representative spectroscopic datasets, their advantages and disadvantages are evaluated, and further improvements are proposed.

2 | MATERIALS AND METHOD

2.1 | Datasets

In this work, SuperCam and RLS representative datasets were used. As described below, the two datasets were obtained analyzing pure mineral phases and Martian-relevant terrestrial analogues by means of representative analytical prototypes.

2.1.1 | RLS-simulated datasets

Leading the development of the RLS system onboard the ExoMars rover, the ERICA group assembled a laboratory prototype that closely emulates the operational mode and the scientific outcome of the Raman instrument onboard the Rosalind Franklin rover. Known as RLS ExoMars Simulator (RLS-Sim), the main characteristics of the prototype have been recently presented.[53] In brief, the RLS-Sim is composed of a continuous laser source emitting at 532 nm, a high-resolution TE Cooled CCD Array spectrometer, an optical head with a long WD objective of 50X. The range of analysis (70–4,200 cm^{-1}), working distance (≈ 15 mm), laser power output (20 mW), spot of analysis (≈50 μm), spectral resolution (6–10 cm^{-1}), and signal to noise ratio of this instrument closely resemble those of the RLS instrument. Software-wise, the RLS ExoMars Simulator integrates the same algorithms implemented by the RLS to autonomously operate on Mars, such as dark subtraction, fluorescence quenching, and acquisition parameters optimization.[59] As proven in previous works, this instrument represents the key analytical tool for the RLS science team to investigate the potential scientific capability of the flight model that will operate on Mars.[60–63] In this work, the RLS-Sim has been used to generate representative Raman datasets (between 20 and 39 spectra automatically collected from each powdered target) from both mineral mixtures (modeling sub-dataset) and terrestrial analogue materials (testing sub-dataset). With regards to the modeling sub-data set, samples of known concentration were created by mixing pure mineral phases from the Analytical Database of Martian Minerals (ADaMM) database.[64] The chemometric model was then tested using Raman data from terrestrial analogue materials selected from the Planetary Terrestrial Analogue Library (PTAL).[65,66]

2.1.2 | SuperCam-simulated datasets

As explained in the introduction section, the SuperCam instrument onboard the Perseverance rover is capable to investigate remote targets through a combination of multiple spectroscopic measurements (Raman, VISIR, LIBS, and Luminescence). In this work, we focused on improving the capability of SuperCam to discriminate mineral phases by developing a data fusion model that combines time-resolved Raman spectra with complementary LIBS data. As such, the analyzed dataset was built using a laboratory prototype named SimulCam.[67] Assembled by the ERICA research group to simulate SuperCam data products, Simulcam is a remote Raman-LIBS system equipped with a Nd:YAG laser, frequency-doubled to provide a 532 nm excitation source. LIBS analyses were carried out by setting a pulse length of 6 ns and 60 mJ energy. The laser is focused on the target with a 50 mm lens, and the emissions by the plasma plume are collected by an Andor Mechelle500 spectrograph (with iStar Andor iCCD camera with integrated DDG) that provides simultaneous recording of the wavelength range between 200 and 975 nm in a single acquisition. Concerning Raman analyses, the laser is delivered to the sample collimated, providing a constant irradiance with distance. The Raman emission of the targeted sample is collected by an SLR Lens (300 mm focal, f: 4–5 mm) and delivered to a two-track spectrometer covering a range between 100 and 4,000 cm^{-1}. The mean spectral resolution of the instrument is

10 cm^{-1}, while laser output has been optimized to obtain remote Raman spectra with an SNR comparable to the SuperCam instrument. Its first use as terrestrial simulator of the Mars 2020 remote spectrometer has been recently presented elsewhere.[68,69] For this work, SimulCam was used to analyze pure carbonates at 3 m distance and under terrestrial temperature and pressure conditions. Selected from the ADaMM database,[64] the analyzed mineral phases are described in Section 3.2.

2.2 | Data treatment and modeling

Prior to data analysis and modeling, all Raman and LIBS spectra were pre-treated using the Instrument Data Analysis Tool (IDAT)/SpectPro software. As presented elsewhere,[70,71] SpectPro was developed by the University of Valladolid to receive, decodify, calibrate, and verify the telemetries generated by the RLS instrument on Mars. The software provides access to an extended set of analytical tools for spectral analysis such as labeling, trimming, shifting, normalization, baseline correction, and features a general-purpose spectrum calculator to perform lineal combinations, product, division and derivative of spectra. Using SpectPro, Raman datasets were baseline-corrected, smoothed and their intensity normalized to one. Furthermore, knowing the quantum efficiency of CCD detectors varies with the wavelength (being the optimal value reached between 400 and 680 nm), the intensity of all spectra was corrected by dividing, for the same wavenumbers, the intensity of the sample spectrum by the intensity of a reference standard (amorphous zinc borate, $Zn_3B_6O_{12}{\cdot}3{,}5H_2O$).[72] Concerning LIBS dataset, no intensity correction was required, so that spectra were only submitted to normalization.

After treatment, SuperCam and RLS datasets were modeled by using two different software. On one side, different data fusion strategies were tested on SuperCam data sets by using a multivariate method based on Principal Component Analysis (PCA).[73] To do so, the Unscrambler®7.6 software was used. On the other side, a dedicated code was created for the semi-quantification of RLS datasets. In this case, all the calculations were performed using MATLAB R2019a.[74]

3 | RESULTS

3.1 | Chemometric models to optimize the scientific return of ExoMars/RLS spectra

Compared to SuperCam and SHERLOC instruments onboard the Nasa Mars2020 rover, the main advantage of the ExoMars RLS spectrometer is the capability to investigate between 20 and 39 spot of interest from powdered samples. As such, the nominal Raman datasets to be acquired on Mars will offer the unique opportunity to fully disclose the mineralogical heterogeneities of the geological samples collected from the subsoil of Oxia Planum.

In this context, a few works have been recently proposed, in which the molecular data gathered by the RLS-Sim from powdered terrestrial analogues is compared to the mineralogical results provided by a commercial X-ray diffractometer.[63,75]

As a representative example,[75] the multi-analytical study of basaltic lava from Reykjanes (Terrestrial analogues of Martian olivine-bearing rocks) proved the multi-point Raman analysis of powdered samples could effectively identify all the main mineral phases composing the samples (diopside, augite, forsterite, and anorthite), while detecting further minor compounds that were below the detection limit of the XRD (calcite, amorphous carbon, and apatite, depending on the sample).

Besides providing a qualitative assessment of the mineralogical composition of a geological sample, tailored chemometric tools are being developed so that RLS datasets could be used to extrapolate a semi-quantitative estimation of the main mineral phases.

Learning from these applications, a reliable semi-quantification of solid mineral mixtures is often achieved using external calibration curves. Knowing there is a linear correlation between the intensity of the Raman signal and the concentration of the mineral phase,[76] a set of samples mixtures is generally prepared by mixing standard minerals at known concentration ratio. All samples are then homogenized (often by grinding) and characterized by setting equal acquisition parameters (modeling sub-data set). After calculating the intensity of the main Raman peaks, binary calibration curves are built in which the ratio between peak intensities of the two mineral phases are plotted against the concentration ratio measured during sample preparation. The equation describing the line or curve that best fits the obtained data distribution is then used to convert the intensity values of Raman spectra collected from the unknown

sample (testing sub-data set) into estimated concentration values. Considering the heterogeneous distribution of mineral phases within geological samples (partially minimized when analyzing powdered materials) and the reduced spot size of Raman spectrometers (≈ 50 μm for the RLS), multiple analyses are necessary in order to achieve a reliable semi-quantitative characterization of the unknown sample. Using this method, several works describe the successful application of Raman spectroscopy to the semi-quantification of binary mineral mixtures, such as calcium oxalate/hydroxyapatite,[77] dolomite/calcite,[78] calcium sulfate/potassium nitrate.[76] By applying binary calibration curves to the chemometric analysis of Raman spectra of more complex mixtures, Kristova et al.[79] successfully quantified quaternary mineral mixtures (hydromagnesite/huntite/dolomite/magnesite).

Focusing on the field of planetary exploration, the chemometric analysis of RLS datasets as a tool to provide a Raman semi-quantification of mineral mixtures on Mars was first postulated by Lopez-Reyes et al.[62] In that work, pure calcite and gypsum powders were mixed at different concentration ratio (ranging from 0.01:0.99 to 0.99:0.01), and 30 spectra per sample were randomly acquired through the RLS-Sim by simulating the operational constraints of the RLS system on Mars. By applying the classical linear Partial Least Squares (PLS) regression method, the measured intensity ratio between the main peaks of calcite (1,086 cm^{-1}) and gypsum (1,008 cm^{-1}) was found to be statistically coherent with real concentration values (r^2 values of the calibration curves ≥0.99, with an average standard deviation ≈3%), thus suggesting the chemometric analysis of RLS datasets could be used to perform semi-quantitative analysis of mineral mixtures.

Following the research line opened by Lopez-Reyes et al.,[62] the RLS science team has been working in the development of tailored semi-quantification methods that could be used to optimize the scientific return of the Raman spectrometer when operating on Mars. In this context, the chemometric method tested in 2013 was recently applied to the study of mineralogical samples having strong analogies with the geological units that are expected to be analyzed by the ExoMars rover on Mars. For instance, the work of Veneranda et al.[80] presented the use of external calibration curves (also based on PLS) to estimate the olivine/pyroxene concentration ratio from ultramafic dunite and pyroxenite samples, these being terrestrial analogues of the ultramafic igneous rocks detected from orbit at the landing site (Oxia Planum).[81,82] As for the work of Lopez-Reyes et al.,[62] external calibration curves were built by analyzing (39 spectra per sample) binary mixtures of olivine/pyroxene at different concentration ratio and analyzed by the RLS-Sim spectrometer. The equations obtained from the chemometric analysis of modeling sub-datasets were then applied to the testing datasets collected from the terrestrial analogues. Raman semi quantitative result were finally compared to XRD reference data (XRD quantification values were calculated using the reference intensity ratio from pattern matching results with XPowder 2004.04.7136[83]). Besides confirming the reliability of the method, this work focused on correlating the semi quantification uncertainty with the size of the employed Raman dataset (ranging from 1 to 39 spectra per sample). As shown in Figure 1, the proportion uncertainty strongly decreases starting from the analysis of 18 spectra, thus suggesting the Raman semi quantification of Martian samples could be achieved when working within the foreseen operational parameters of RLS (between 20 and 39 spots).

Inspired by the work of Kristova et al.,[79] binary calibration curves were also used to semi-quantify terrestrial analogues of higher mineralogical complexity. Being the main components of Martian basaltic rocks, Veneranda et al.[84] prepared binary mixtures of lepidocrocite, augite, and forsterite phases. The obtained Raman calibration curves were then used to semi-quantify ternary mixtures of feldspar, pyroxene, and olivine minerals. As displayed in Figure 2, the obtained Raman semi-quantification results were in good with real concentration values. Thanks to this comparison, it was also proved the proposed chemometric model tends to underestimate the concentration of feldspar phases, especially when the collected spectra display a high variability in the intensity of the fluorescence background. To improve the reliability of the results, the RLS science team is evaluating the factors affecting the fluorescence (e.g., granulometry) and the magnitude of their influence in the variation of Raman peaks intensities.

Following this line of study, members of the RLS team recently extended the use of external calibration curves to the Raman semi-quantification of organo-mineral mixtures. In detail, Demaret et al.[85] presented optimized calibration curves in which the relation between peak intensity ratios and real concentration values have been improved by the introduction of a correction factor that takes into account the apparent Raman scattering coefficient of the analyzed compounds. Using this method, the concentration ratio of calcite-gypsum mineral mixtures spiked with amino acids (L-Cysteine) was successfully achieved. Beyond improving the mineralogical characterization of geological samples, this proves the chemometric analysis of RLS datasets could also optimize the contribution of RLS for astrobiological investigations.

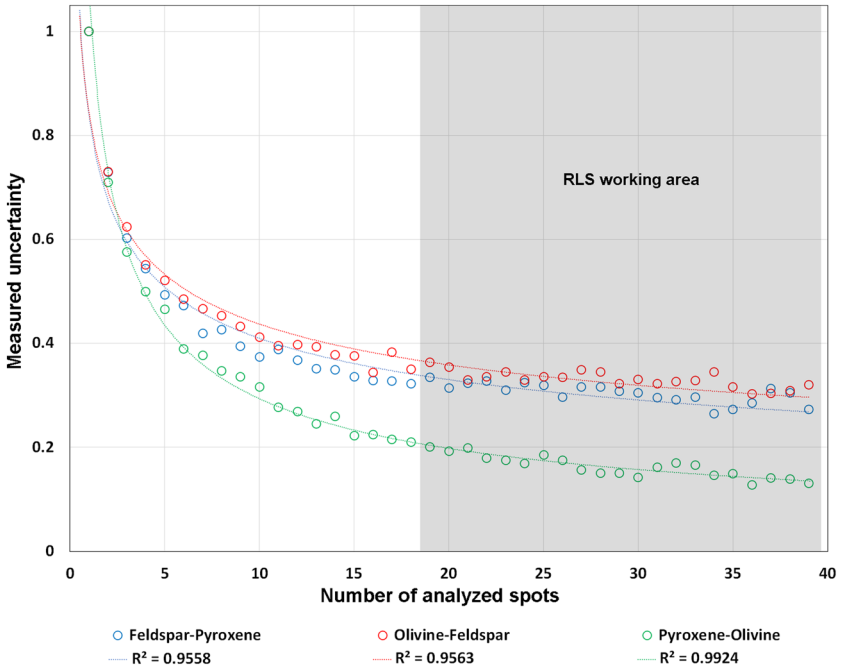

FIGURE 1 Prediction uncertainty of feldspar/pyroxene (blue), olivine/feldspar (red) and pyroxene/olivine (green) binary calibration curves as a function of the number of analyzed spots per line.

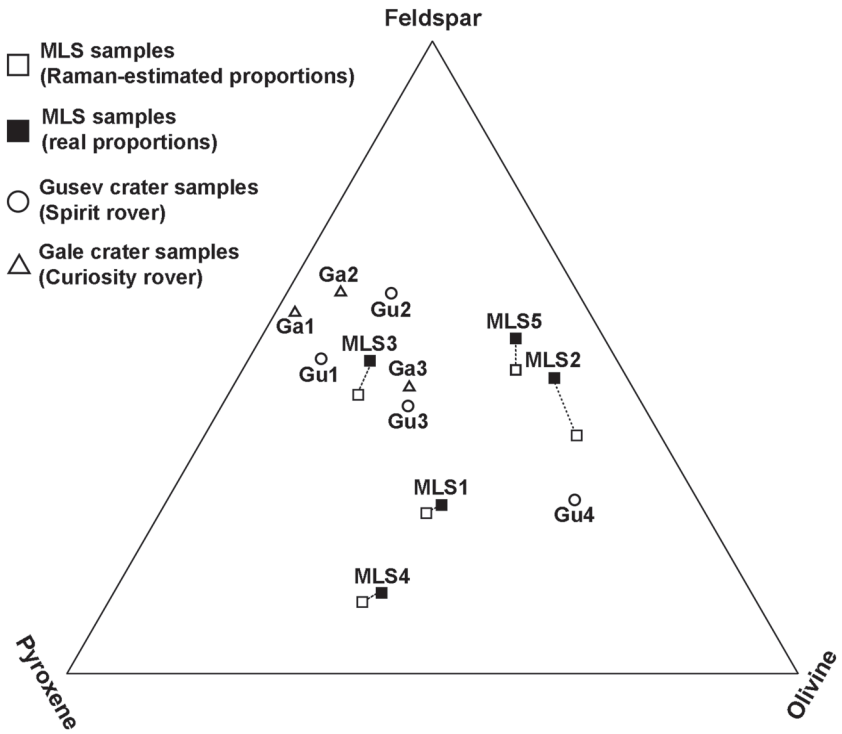

FIGURE 2 Ternary diagram displaying real and calculated phase proportion of ternary mixtures. As reference, feldspar-pyroxene-olivine ratio of Martian basaltic rocks and soils measured by Spirit and Curiosity rovers are also provided (from Veneranda et al.[84]).

Despite the promising results obtained by the mentioned Raman semi-quantification methods, the RLS quantitative analysis of real Martian samples could present additional challenges that need to be addressed. For instance, the uncertainty of the measurement could increase due to the analysis of mineral phases having different degree of crystallinity

or elemental composition (e.g., forsterite vs. fayalite) to the mineral specimens used for the construction of calibration curves. To minimize the potential issues related to the use of (terrestrial) modeling sub-dataset for the chemometric analysis of Raman spectra from Mars, the chemometric model should take into account a wider set of vibrational indicators (e.g., maximum intensity position of additional peaks from different spectroscopic regions as well as their FWHM and intensity ratio). Through the analysis and comparison of the mentioned parameters, correlation coefficients could be elaborated to better adapt Terrestrial external calibration curves to the Raman datasets received from Mars.

3.2 | Chemometric models to optimize the scientific return of Mars 2020/SuperCam spectra

The SuperCam instrument is a multi-analytical suite that combines microphone recordings with the spectroscopic VISIR, LIBS, Raman and luminescence investigation of remote targets. As explained elsewhere, SuperCam is a highly evolved version of the ChemCam LIBS instrument onboard the Curiosity rover,[86] which is operating on Mars since 2012. Taking advantage of the overwhelming amount of analytical data collected in the past decades (more than 800,000 spectra from over 20,000 observation points[87]), the ChemCam team developed multiple chemometric methods to quantify the major rock forming elements as oxides. As presented elsewhere,[87] the quantification of major elements is based on the use of multivariate models,[88,89] while minor and trace elements are calibrated using a combination of univariate models and peak-fitting methods.[90,91]

Learning from the chemometric analysis of ChemCam data and taking advantage of the large number of on-board SuperCam calibration targets (that cover a greater compositional range than ChemCam[19]), tailored chemometric models are being developed to optimize the elemental quantification of LIBS data. For instance, Kostantinidis et al.[55] recently described a novel statistical model based on spectral clustering and a linear mixture model for the elemental quantification of LIBS data from planetary missions. Focusing on SuperCam, the work of Anderson et al.[92] presents a set of novel multivariate and univariate calibration models (based on PLS) to quantify major and minor/trace elements detected by SCAM LIBS analysis on Mars.

As the development of chemometric systems for the quantitative analysis of LIBS spectra is at a relatively advanced stage, the greatest analytical challenge provided by SuperCam consists in combining the interpretation of LIBS data with the results gathered by complementary spectroscopic systems from the same spot of interest (e.g., Raman, VISIR, and luminescence). As highlighted in the literature, data fusion strategies have been successfully applied in several terrestrial applications[49,50,93–96] to enhance the exploitation of complementary spectroscopic data. Focusing on the field of space exploration, most of the few manuscripts published to date present the combination Raman-LIBS spectra based on the low-level chemometric strategies.[58,97–99] For instance, knowing that epsomite, anhydrous sodium sulfate, and hexahydrate magnesium chloride are widely present on both Mars and Europa (Jupiter's satellite), Manrique-Martinez et al.[97] achieved a reliable semi-quantification of their binary mixtures by developing a tailored multivariate strategy that combines PCA, with artificial neural networks (ANN). Focusing on optimizing the exploitation of SuperCam data, the method proposed by Rammelkamp et al.[58] combines PCA and partial least squares discriminant analysis (PLS-DA) to evaluate the advantages provided by the fusion of LIBS and Raman spectra in the discrimination of unknown geological targets.

To support the SuperCam science team, the ERICA research group is evaluating and comparing the capability of several data fusion strategies to improve the multi-analytical discrimination of mineral phases on Mars. As a representative example, the SimulCam laboratory simulator has been recently used to perform remote spectroscopic analysis of carbonate minerals within the Ca-Mg-Fe ternary diagram. In detail, calcite ($CaCO_3$), aragonite ($CaCO_3$), dolomite (CaMg $[CO_3]_2$), huntite (CaMg3$[CO_3]_4$), magnesite ($MgCO_3$), siderite ($FeCO_3$), and ankerite (Mg,Fe $[CO_3]_2$) mineral samples were selected from the ADaMM mineral database. After powdering and pellet preparation, a set of 5 Raman and LIBS spectra per sample were collected at a representative distance (3 m) by trying to closely simulate the acquisition parameters of the SuperCam instrument. After baseline correction and normalization, each Raman spectrum (4,000 channels) was attached to the LIBS spectrum (16,000 channels, collected from the same spot of analysis) to obtain a single spectral file (20,000 channels) (see Figure 3).

By performing the same procedure to all the analyzed spots, a data matrix with a total size of 20,000 columns (as the number of total channels for each combined Raman-LIBS spectra) and 35 rows (given as the number of analyzed spot per sample multiplied by the number of total samples) was obtained. The PCA of the Raman-LIBS data matrix was then performed using the Unscrambler software, and the results compared with those provided by the PCA of Raman

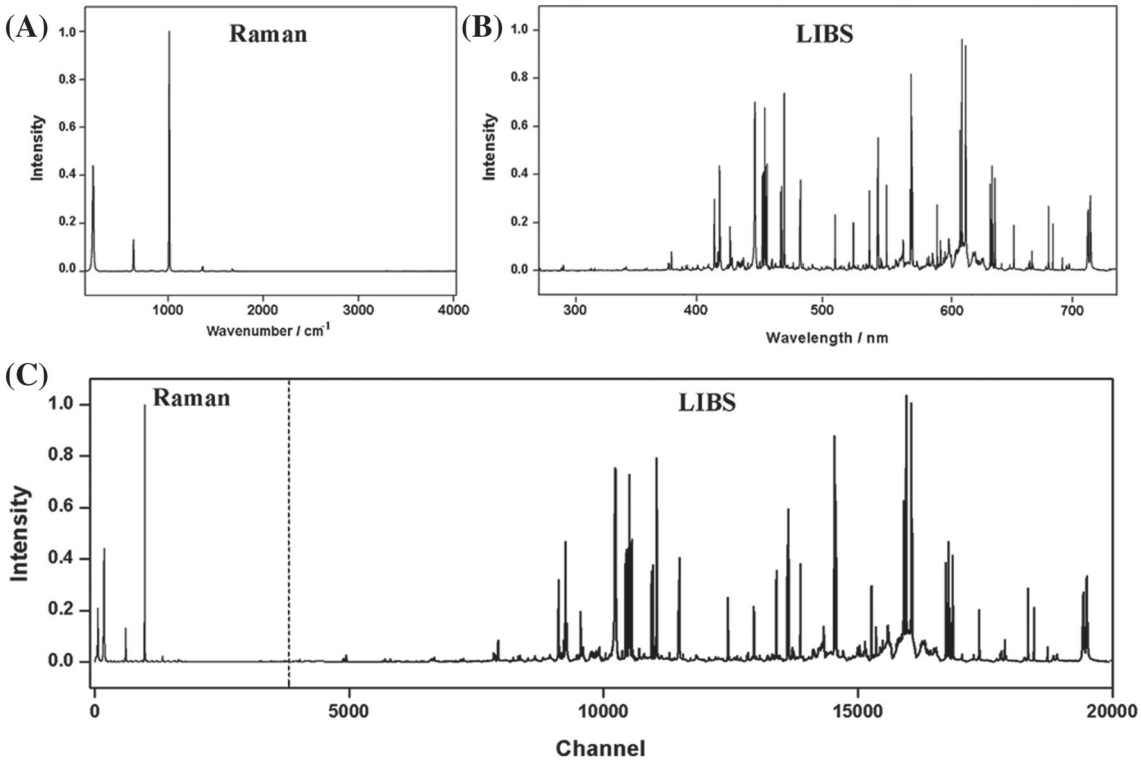

FIGURE 3 (A) baseline-corrected Raman spectra, (B) LIBS spectra, and (C) low-level fused Raman-LIBS spectra collected from the calcium carbonate sample.

spectra and LIBS spectra alone. As presented in Figure 4, 3D graphs were created to represent the three main Principal Components (PC1, PC2, and PC3) along the *X*, *Y*, and *Z* axes, respectively.

The Euclidean distance between the average points of each mineral phase in the PC1, PC2, PC3 three-dimensional space was calculated by using the following equation:

$$\mathrm{ED}(\mathrm{a},\mathrm{b}) = \sqrt{(\mathrm{PC1_b} - \mathrm{PC1_a})^2 + (\mathrm{PC2_b} - \mathrm{PC2_a})^2 + (\mathrm{PC3_b} - \mathrm{PC3_a})^2},$$

where *a* and *b* being the average points of two mineral clusters and PC1, PC2, and PC3 the main principal components describing the variance of the data. The measured ED are represented in Table 1.

Knowing the discrimination capability between two mineral phases is directly related to the Euclidean distance between their clusters (together with their size), the results summarized in Table 1A suggests PCA based on LIBS results effectively discriminate most of the carbonate phases within the Ca-Mg-Fe ternary phases, having the lower ED values measured between aragonite-calcite (ED = 0.38), dolomite-aragonite (0.47) and ankerite-dolomite (0.21) clusters. Similarly, the lower ED extrapolated from the PCA of Raman results (Table 1B) were calculated between aragonite-calcite (0.32), siderite-calcite (0.50) and ankerite-dolomite (0.27) clusters.

The results obtained from LIBS and Raman spectra were finally compared to the ED measured from the PCA of the combined Raman-LIBS data matrix. As represented in Table 1C, most of the measured ED was higher than both mono-analytical approaches. Knowing the variation on cluster sizes was negligible, this comparison clearly proved the chemometric analysis of low-level combined Raman-LIBS data could increase the capability of the SimulCam instrument to discriminate carbonate phases. Besides low-level strategies, the mid-level combination of spectroscopic data returned by the SuperCam instrument are also being evaluated. The preliminary results of this extensive work will be soon described in a dedicated paper.

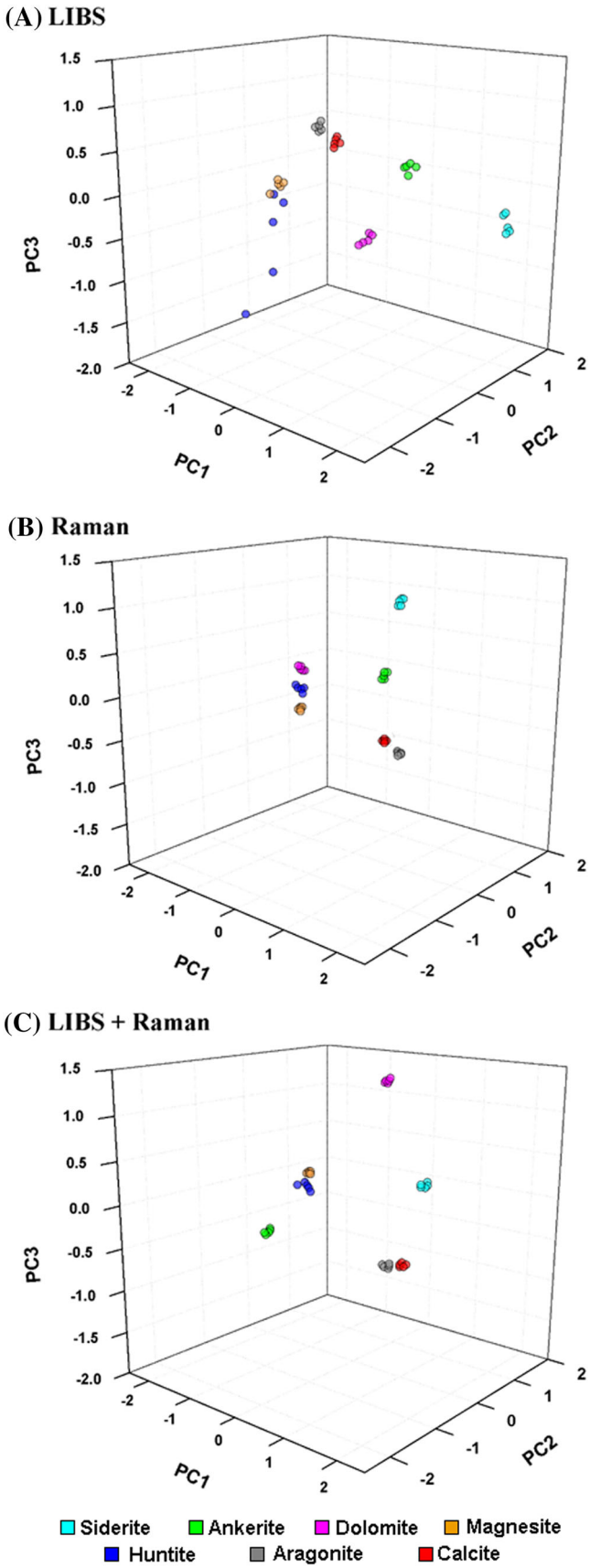

FIGURE 4 Three-dimensional graph representing how the different mineral clusters are discriminated by considering PC1, PC2, and PC3 values obtained from the PCA analysis of Raman (A), LIBS (B), and Raman + LIBS (C) data matrixes.

TABLE 1 ED measured between mineral clusters from the PCA of LIBS (A), Raman (B), and fused LIBS-Raman (C) spectra

	ED	CAL	ARG	DOL	HUN	MAG	SID	ANK
A. LIBS	**CAL**	0.00						
	ARG	0.38	0.00					
	DOL	0.83	0.47	0.00				
	HUN	1.26	1.05	0.77	0.00			
	MAG	2.00	1.85	1.63	0.89	0.00		
	SID	2.03	1.85	1.77	1.66	1.69	0.00	
	ANK	0.89	0.56	0.21	0.61	1.45	1.60	0.00
B. Raman	**ED**	**CAL**	**ARG**	**DOL**	**HUN**	**MAG**	**SID**	**ANK**
	CAL	0.00						
	ARG	0.32	0.00					
	DOL	1.79	1.96	0.00				
	HUN	1.73	1.73	2.03	0.00			
	MAG	2.05	1.95	1.70	2.30	0.00		
	SID	0.50	0.70	1.60	2.09	1.97	0.00	
	ANK	1.64	1.80	0.27	2.07	1.52	1.41	0.00
C. Raman-LIBS	**ED**	**CAL**	**ARG**	**DOL**	**HUN**	**MAG**	**SID**	**ANK**
	CAL	0.00						
	ARG	0.19	0.00					
	DOL	1.81	1.85	0.00				
	HUN	1.87	1.71	2.21	0.00			
	MAG	2.82	2.76	2.17	2.06	0.00		
	SID	1.94	1.95	2.53	2.72	2.30	0.00	
	ANK	1.75	1.79	0.40	2.15	1.88	2.18	0.00

Increased over both techniques
Increased over one technique
Decreased over one technique
Decreased over both techniques

4 | CONCLUSIONS

This work provides an updated overview on the chemometric tools the scientific community is developing with the purpose of optimizing the scientific outcome of the Raman spectra returned from planetary exploration missions. Besides providing a review of the main chemometric models that are expecting to enhance the exploitation of SuperCam and RLS data, this manuscript presents the chemometric solution the ERICA research group is developing for both spectroscopic instruments. Focusing on the interpretation of RLS spectra, the information here provided suggests the datasets the RLS will collect from powdered subsoil material (between 20 and 39 spectra per sample) could be used to semi-quantify the main mineral phases of a geological matrix. So far, uni- and multi-variate chemometric models based on the use of external calibration curves (based on PLS) have been applied to semi-quantification of both synthetic mineral mixtures and natural terrestrial analogue samples. The reliability of Raman results was in line with reference XRD data, thus suggesting that Raman spectroscopy could be effectively used to perform semi-quantitative analysis on Mars. Despite the promising results, further developments need to be addressed in the future to increase the robustness of the proposed semi-quantification models. For instance, the analysis of a wider set of vibrational indicators (see Section 3.1) could minimize the issues related to the use of calibration curves made from the analysis of Terrestrial mineral mixtures

for the semi-quantification of Raman datasets from Mars. In this case, complementary chemometric model will be evaluated, in which the predictive ability of the ANN (coupled to PCA) will be compared to the PLS regression method used so far. Further chemometric models are being tested to increase the capability of the SuperCam instrument to discriminate mineral phases. As SuperCam can interrogate the same spot of interest with multiple spectroscopic techniques, the ERICA research group is evaluating the advantages provided by the data fusion of Raman-LIBS data. In this framework, the preliminary results of the proposed low-level data combination strategy (based on PCA) prove the discrimination capability among Ca-Mg-Fe carbonate phases strongly increase when fused Raman-LIBS spectra are considered. As this is just the first attempt towards the development of a SuperCam-dedicated data fusion strategy, further methods also need to be evaluated and compared. The next step consists in the application of a mid-level data fusion method, in which the fusion of raw spectra will be replaced by the combination of pre-selected spectroscopic indicators (e.g the wavelength position of Raman peaks and the intensity value of selected LIBS emission lines). Considering the lessons learnt from terrestrial applications, and in light of the encouraging results obtained so far from the analysis of simulated SuperCam and RLS datasets, the development of tailored chemometric models clearly represents a promising approach to optimize the scientific outcome of Raman data returned from Mars.

ACKNOWLEDGMENTS

This work is financed through the European Commission through the H2020- COMPET-2015 programme (Grant 687302) and the Ministry of Economy and Competitiveness (MINECO, Grant PID2019-107442RBC31).

PEER REVIEW

The peer review history for this article is available at https://publons.com/publon/10.1002/cem.3438.

DATA AVAILABILITY STATEMENT

The data presented in this manuscript will be made available on genuine request.

ORCID

Marco Veneranda https://orcid.org/0000-0002-7185-2791
Jose Antonio Manrique https://orcid.org/0000-0002-2053-2819
Menelaos Konstantinidis https://orcid.org/0000-0002-5074-9023
Guillermo Lopez-Reyes https://orcid.org/0000-0003-1005-1760

REFERENCES

1. Economou T. Chemical analyses of Martian soil and rocks obtained by the pathfinder alpha proton X-ray spectrometer. *Radiat Phys Chem*. 2001;61(3-6):191-197. doi:10.1016/S0969-806X(01)00240-7
2. Arvidson RE, Squyres SW, Anderson RC, et al. Overview of the Spirit Mars Exploration Rover Mission to Gusev Crater: landing site to Backstay Rock in the Columbia Hills. *J Geophys Res E Planets*. 2006;111:1-22.
3. Squyres SW, Arvidson RE, Bollen D, et al. Overview of the opportunity Mars Exploration Rover Mission to Meridiani Planum: Eagle Crater to Purgatory Ripple. *J Geophys Res E Planets*. 2006;111:1-19.
4. Gellert R, Rieder R, Brückner J, et al. Alpha particle X-ray spectrometer (APXS): results from Gusev crater and calibration report. *J Geophys Res E Planets*. 2006;111(E2). doi:10.1029/2005JE002555
5. Morris RV, Klingelhöfer G, Bernhardt B, et al. Mineralogy at Gusev crater from the Mössbauer spectrometer on the Spirit rover. *Science (80-)*. 2004;305(5685):833-836. doi:10.1126/science.1100020
6. Klingelhöfer G, Morris RV, Bernhardt B, et al. Jarosite and hematite at Meridiani Planum from opportunity's Mössbauer spectrometer. *Science (80-)*. 2004;306(5702):1740-1745. doi:10.1126/science.1104653
7. Christensen PR, Wyatt MB, Glotch TD, et al. Mineralogy at Meridiani Planum from the Mini-TES experiment on the opportunity rover. *Science (80-)*. 2004;306(5702):1733-1739. doi:10.1126/science.1104909
8. Harri AM, Genzer M, Kemppinen O, et al. Pressure observations by the curiosity rover: initial results. *J Geophys Res E Planets*. 2014; 119(1):82-92. doi:10.1002/2013JE004423
9. Thompson LM, Schmidt ME, Spray JG, et al. Potassium-rich sandstones within the Gale impact crater, Mars: the APXS perspective. *J Geophys Res Planets*. 2016;121(10):1981-2003. doi:10.1002/2016JE005055
10. Bish D, Blake D, Vaniman D, et al. The first X-ray diffraction measurements on Mars. *IUCrJ*. 2014;1(6):514-522. doi:10.1107/S2052252514021150
11. Maurice S, Wiens RC, Saccoccio M, et al. The ChemCam instrument suite on the Mars Science Laboratory (MSL) rover: science objectives and mast unit description. *Space Sci Rev*. 2012;170(1-4):95-166. doi:10.1007/s11214-012-9912-2

12. Downs RT. Determining mineralogy on mars with the CheMin X-ray diffractometer. *Elements*. 2015;11(1):45-50. doi:10.2113/gselements.11.1.45
13. Grotzinger JP, Crisp JA, Vasavada AR. Curiosity's mission of exploration at gale crater, mars. *Elements*. 2015;11(1):19-26. doi:10.2113/gselements.11.1.19
14. Vago JL, Coates AJ, Jaumann R, et al. Searching for traces of life With the ExoMars Rover. In: *From Habitability to Life on Mars*. Elsevier Inc; 2018. doi:10.1016/b978-0-12-809935-3.00011-6.
15. Farley KA, Williford KH, Stack KM, et al. Mars 2020 Mission overview. *Space Sci Rev*. 2020;216(8):142. doi:10.1007/s11214-020-00762-y
16. Beegle L, Bhartia R, White M, DeFlores L, Abbey W, Wu YH, Cameron B, Moore J, Fries M, Burton A, Edgett KS SHERLOC: Scanning habitable environments with Raman & luminescence for organics & chemicals. in IEEE Aerospace Conference Proceedings 1–11 2015. 10.1109/AERO.2015.7119105.
17. Maurice S, Wiens RC, Bernardi P, et al. The SuperCam instrument suite on the Mars 2020 rover: science objectives and mast-unit description. *Space Sci Rev*. 2021;217(3):47. doi:10.1007/s11214-021-00807-w
18. Wiens RC, Maurice S, Robinson SH, et al. The SuperCam instrument suite on the NASA Mars 2020 rover: body unit and combined system tests. *Space Sci Rev*. 2021;217(1):1-87. doi:10.1007/s11214-020-00777-5
19. Manrique JA, Lopez-Reyes G, Cousin A, et al. SuperCam calibration targets: design and development. *Space Sci Rev*. 2020;216:1-27.
20. Rull F, Maurice S, Hutchinson I, et al. The Raman laser spectrometer for the ExoMars rover mission to Mars. *Astrobiology*. 2017;17(6-7):627-654. doi:10.1089/ast.2016.1567
21. Bibring JP, Hamm V, Pilorget C, Vago JL, Team, M. The MicrOmega investigation onboard ExoMars. *Astrobiology*. 2017;17(6-7):621-626. doi:10.1089/ast.2016.1642
22. Goesmann F, Brinckerhoff WB, Raulin F, et al. The Mars Organic Molecule Analyzer (MOMA) instrument: characterization of organic material in Martian sediments. *Astrobiology*. 2017;17(6-7):655-685. doi:10.1089/ast.2016.1551
23. Schröder S, Belenguer T, Böttger U, Buder M, Cho Y, Dietz E, Gensch M, Hagelschuer T, Hanke F, Hübers HW, Kameda S. In-situ Raman spectroscopy on Phobos: RAX on the MMX rover. in 51st Lunar and Planetary Science Conference 2019. 10.5840/dspl20203218, 2020; 3(2): 75, 95.
24. Ulamec S, Michel P, Grott M, Böttger U, Heinz-Wilhelm Hübers NM, Vernazza P, Karatekin Ö, Knollenberg J, Willner K, Grebenstein M, Mary S, Chazalnoël P, Biele J, Krause C, Ho TM, Lange C, Grundmann JT, Sasaki K, Maibaum M, Küchemann O, Jose FR. A rover for the JAXA MMX Mission to Phobos. in 70th International Astronautical Congress 1–8 2019.
25. Phillips CB, Hand KP, Cable ML, Hofmann AE, Craft KL. Updates on the Europa Lander Mission Concept. in 50th Lunar and Planetary Science Conference 2685. 2019. 10.1130/abs/2018am-324050.
26. Sharma SK, Porter JN, Misra AK, Acosta-Maeda TE, Angel SM, McKay CP. Standoff Raman spectroscopy for future Europa Lander missions. *J Raman Spectrosc*. 2020;51(9):1782-1793. doi:10.1002/jrs.5814
27. Tallarida N, Lambert J, Wang A. Fluorescence mitigation using the Compact Integrated Raman Spectrometer (CIRS) for in situ analysis of minerals and organics. in 49th Lunar and Planetary Science Conference 2018.
28. Asri MNM, Nestrgan NF, Nor NAM, Verma R. On the discrimination of inkjet, laser and photocopier printed documents using Raman spectroscopy and chemometrics: application in forensic science. *Microchem J*. 2021;165:106136. doi:10.1016/j.microc.2021.106136
29. Khandasammy SR, Fikiet MA, Mistek E, et al. Bloodstains, paintings, and drugs: Raman spectroscopy applications in forensic science. *Forensic Chem*. 2018;8:111-133. doi:10.1016/j.forc.2018.02.002
30. Levermore JM, Smith TEL, Kelly FJ, Wright SL. Detection of microplastics in ambient particulate matter using Raman spectral imaging and chemometric analysis. *Anal Chem*. 2020;92(13):8732-8740. doi:10.1021/acs.analchem.9b05445
31. Marchetti M, Offroy M, Abdat F, et al. Chemometrics-assisted monitoring in Raman spectroscopy for the biodegradation process of an aqueous polyfluoroalkyl ether from a fire-fighting foam in an environmental matrix. *Environments*. 2020;7:1-14.
32. Peris-Díaz MD, Łydżba-Kopczyńska B, Sentandreu E. Raman spectroscopy coupled to chemometrics to discriminate provenance and geological age of amber. *J Raman Spectrosc*. 2018;49(5):842-851. doi:10.1002/jrs.5357
33. Wiggins MB, Liu M, Liu C, Booksh KS. Polymorph identification in green Chinese architectural paints using Raman imaging and multivariate curve resolution. *J Chemometr*. 2021;35(1):1-10. doi:10.1002/cem.3308
34. Kwofie F, Lavine BK, Ottaway J, Booksh K. Incorporating brand variability into classification of edible oils by Raman spectroscopy. *J Chemometr*. 2020;34(7):1-14. doi:10.1002/cem.3173
35. Dong J, Hong M, Xu Y, Zheng X. A practical convolutional neural network model for discriminating Raman spectra of human and animal blood. *J Chemometr*. 2019;33(11):1-12. doi:10.1002/cem.3184
36. Vajna B, Patyi G, Nagy Z, Bódis A, Farkas A, Marosi G. Comparison of chemometric methods in the analysis of pharmaceuticals with hyperspectral Raman imaging. *J Raman Spectrosc*. 2011;42(11):1977-1986. doi:10.1002/jrs.2943
37. Farkas A, Nagy B, Démuth B, et al. Variable clustering and spectral angle mapper-orthogonal projection method for Raman mapping of compound detection in tablets. *J Chemometr*. 2017;31(1):1-11. doi:10.1002/cem.2861
38. Taleb A, Diamond J, McGarvey JJ, Beattie JR, Toland C, Hamilton PW. Raman microscopy for the chemometric analysis of tumor cells. *J Phys Chem B*. 2006;110(39):19625-19631. doi:10.1021/jp061981q
39. Dörfer T, Bocklitz T, Tarcea N, Schmitt M, Popp J. Checking and improving calibration of raman spectra using chemometric approaches. *Zeitschrift fur Phys Chemie*. 2011;225(6-7):753-764. doi:10.1524/zpch.2011.0077
40. Li Q, Sun X, Ma X, et al. A calibration transfer methodology for standardization of Raman instruments with different spectral resolutions using double digital projection slit. *Chemom Intel Lab Syst*. 2019;191:143-147. doi:10.1016/j.chemolab.2019.07.004

41. Carneiro CR, Silva CS, de Carvalho MA, Pimentel MF, Talhavini M, Weber IT. Identification of luminescent markers for gunshot residues: fluorescence, Raman spectroscopy, and chemometrics. *Anal Chem*. 2019;91(19):12444-12452. doi:10.1021/acs.analchem.9b03079
42. Senger RS, Scherr D. Resolving complex phenotypes with Raman spectroscopy and chemometrics. *Curr Opin Biotechnol*. 2020;66:277-282. doi:10.1016/j.copbio.2020.09.007
43. Schumacher W, Kühnert M, Rösch P, Popp J. Identification and classification of organic and inorganic components of particulate matter via Raman spectroscopy and chemometric approaches. *J Raman Spectrosc*. 2011;42(3):383-392. doi:10.1002/jrs.2702
44. Luna AS, da Silva AP, da Silva CS, Lima ICA, de Gois JS. Chemometric methods for classification of clonal varieties of green coffee using Raman spectroscopy and direct sample analysis. *J Food Compos Anal*. 2019;76:44-50. doi:10.1016/j.jfca.2018.12.001
45. Li B, Calvet A, Casamayou-Boucau Y, Morris C, Ryder AG. Low-content quantification in powders using Raman spectroscopy: a facile chemometric approach to sub 0.1% limits of detection. *Anal Chem*. 2015;87(6):3419-3428. doi:10.1021/ac504776m
46. Richardson PIC, Muhamadali H, Ellis DI, Goodacre R. Rapid quantification of the adulteration of fresh coconut water by dilution and sugars using Raman spectroscopy and chemometrics. *Food Chem*. 2019;272:157-164. doi:10.1016/j.foodchem.2018.08.038
47. Jiménez-Carvelo AM, Osorio MT, Koidis A, González-Casado A, Cuadros-Rodríguez L. Chemometric classification and quantification of olive oil in blends with any edible vegetable oils using FTIR-ATR and Raman spectroscopy. *LWT*. 2017;86:174-184. doi:10.1016/j.lwt.2017.07.050
48. Ghosh A, Raha S, Dey S, Chatterjee K, Roy Chowdhury A, Barui A. Chemometric analysis of integrated FTIR and Raman spectra obtained by non-invasive exfoliative cytology for the screening of oral cancer. *Analyst*. 2019;144(4):1309-1325. doi:10.1039/C8AN02092B
49. Hoehse M, Paul A, Gornushkin I. Multivariate classification of pigments and inks using combined Raman spectroscopy and LIBS. *Anal Bioanal Chem*. 2012;402(4):1443-1450. doi:10.1007/s00216-011-5287-6
50. Shameem KMM, Choudhari KS, Bankapur A. A hybrid LIBS—Raman system combined with chemometrics: an efficient tool for plastic identification and sorting. *Anal Bioanal Chem*. 2017;409(13):3299-3308. doi:10.1007/s00216-017-0268-z
51. Luna AS, Lima ICA, Rocha WFC, et al. Classification of soil samples based on Raman spectroscopy and X-ray fluorescence spectrometry combined with chemometric methods and variable selection. *Anal Methods*. 2014;6(22):8930-8939. doi:10.1039/C4AY01967A
52. Ramos PM, Ruisánchez I, Andrikopoulos KS. Micro-Raman and X-ray fluorescence spectroscopy data fusion for the classification of ochre pigments. *Talanta*. 2008;75(4):926-936. doi:10.1016/j.talanta.2007.12.030
53. Lopez-Reyes G, Veneranda M, Manrique JA, et al. The Raman laser spectrometer ExoMars simulator (RLS Sim): a heavy-duty Raman tool for ground testing on ExoMars. *J Raman Spectrosc*. 2021;53:382-395.
54. Martin PE, Ehlmann BL, Thomas NH, et al. Studies of a lacustrine-volcanic Mars analog field site with Mars-2020-like instruments. *Earth Sp Sci*. 2020;7:1-28.
55. Konstantinidis M, Cote K, Lalla EA, et al. On the application of a novel linear mixture model on laser-induced breakdown spectroscopy: implications for Mars. *J Chemometr*. 2019;33(10):1-15. doi:10.1002/cem.3174
56. Veneranda M, Lopez-Reyes G, Manrique-Martinez JA, et al. ExoMars Raman Laser Spectrometer (RLS): development of chemometric tools to classify ultramafic igneous rocks on Mars. *Sci Rep*. 2020;10(1):16954. doi:10.1038/s41598-020-73846-y
57. Breitenfeld LB, Dyar MD, Carey CJ, et al. Predicting olivine composition using Raman spectroscopy through band shift and multivariate analyses. *Am Mineral*. 2018;103(11):1827-1836. doi:10.2138/am-2018-6291
58. Rammelkamp K, Schröder S, Kubitza S, et al. Low-level LIBS and Raman data fusion in the context of in situ Mars exploration. *J Raman Spectrosc*. 2020;51(9):1682-1701. doi:10.1002/jrs.5615
59. Lopez-Reyes G, Rull Pérez F. A method for the automated Raman spectra acquisition. *J Raman Spectrosc*. 2017;48(11):1654-1664. doi:10.1002/jrs.5185
60. Lalla EA, Lopez-Reyes G, Lozano-Gorrín AD, Rull F. Combined vibrational, structural, elemental and Mössbauer spectroscopic analysis of natural phillipsite (zeolite) from historical eruptions in Tenerife, Canary Islands: implication for Mars. *Vib Spectrosc*. 2019;101:10-19. doi:10.1016/j.vibspec.2018.12.003
61. Veneranda M, Lopez-Reyes G, Saiz J, et al. ExoFiT trial at the Atacama Desert (Chile): Raman detection of biomarkers by representative prototypes of the ExoMars/Raman Laser Spectrometer. *Sci Rep*. 2021;11(1):1461. doi:10.1038/s41598-021-81014-z
62. Lopez-Reyes G, Rull F, Venegas G, et al. Analysis of the scientific capabilities of the ExoMars Raman laser spectrometer instrument. *Eur J Mineral*. 2013;25(5):721-733. doi:10.1127/0935-1221/2013/0025-2317
63. Veneranda M, Lopez-Reyes G, Manrique JA, et al. ExoMars raman laser spectrometer: a tool for the potential recognition of wet-target craters on mars. *Astrobiology*. 2020;20(3):349-363. doi:10.1089/ast.2019.2095
64. Veneranda M, Sanz-Arranz A, Manrique JA, et al. Analytical Database of Martian Minerals (ADaMM): project synopsis and Raman data overview. *J Raman Spectrosc*. 2021;53:364-381.
65. Dypvik H, Hellevang H, Krzesińska A, et al. The Planetary Terrestrial Analogues Library (PTAL)—an exclusive lithological selection of possible Martian earth analogues. *Planet Space Sci*. 2021;208:105339. doi:10.1016/j.pss.2021.105339
66. Veneranda M, Sáiz J, Sanz-Arranz A, et al. Planetary Terrestrial Analogues Library (PTAL) project: Raman data overview. *J Raman Spectrosc*. 2019;1–19(9):1731-1749. doi:10.1002/jrs.5652
67. Rull F, Veneranda M, Manrique-Martinez JA, et al. Analytica Chimica Acta spectroscopic study of terrestrial analogues to support rover missions to Mars e a Raman-centred review. *Anal Chim Acta*. 2021;339003. doi:10.1016/j.aca.2021.339003
68. Veneranda M, Manrique JA, Lopez-Reyes G, Sanz-Arranz A, Saiz J, Navarro R, Medina J, Shkolyar S, Rull F, Maurice S, Wiens RC. Combination of remote Raman-LIBS data: novel mineral discrimination strategies to support SuperCam on Mars. in Lunar and Planetary Science Conference 1 2020.

69. Manrique-Martinez JA, Veneranda M, Lopez-Reyes G, et al. Automatic identification of carbonates based in Raman-LIBS combination. in GeoRaman Congress 2020 52 2020.
70. Saiz J, Lopez-Reyes G, Veneranda M, Manrique JA, Guzmán A, Moreno-Dominguez D, Werner S, Poulet F, Medina J, Rull F. Automated sample identification with SpectPro and PTAL database for the analysis of spectra from planetary missions. in EGU General Assembly 2019, 17904 (2019).
71. Veneranda M, Saiz J, Lopez-Reyes G, Manrique JA, Arranz AS, Garcia-Prieto C, Werner SC, Moral A, Madariaga JM, Medina J, Rull F. PTAL, ADAMM and SpectPro: novel tools to support ExoMars and Mars 2020 science operations. in Europlanet Science Congress 2020.
72. Sanz-Arranz A, Manrique-Martinez JA, Medina-Garcia J, Rull-Perez F. Amorphous zinc borate as a simple standard for baseline correction in Raman spectra. *J Raman Spectrosc*. 2017;48(11):1644-1653. doi:10.1002/jrs.5144
73. Tharwat A. Principal component analysis—a tutorial. *Int J Appl Pattern Recognit*. 2016;3(3):197. doi:10.1504/IJAPR.2016.079733
74. Fisher AAE. An introduction to coding with Matlab: simulation of X-ray photoelectron spectroscopy by employing Slater's rules. *J Chem Educ*. 2019;96(7):1502-1505. doi:10.1021/acs.jchemed.9b00236
75. Veneranda M, Manrique-Martinez JA, Lopez-Reyes G, et al. Spectroscopic study of olivine-bearing rocks and its relevance to the ExoMars rover mission. *Spectrochim Acta - Part a Mol Biomol Spectrosc*. 2019;223:117360. doi:10.1016/j.saa.2019.117360
76. Costantini I, Veneranda M, Prieto-Taboada N, Bellot-Gurlet L, Castro K, Madariaga JM. Comparison of semiquantification experimental methodologies using micro-Raman spectroscopy: Palme software as an alternative tool for the study of salt efflorescence. *J Raman Spectrosc*. 2016;47(12):1415-1421. doi:10.1002/jrs.5057
77. Kontoyannis CG, Bouropoulos NC, Koutsoukos PG, Raman spectroscopy: A tool for the quantitative analysis of mineral components of solid mixtures. The case of calcium oxalate monohydrate and hydroxyapatite, *Vib Spectrosc.* 1997;15(1):53-60. doi:10.1016/S0924-2031(97)00025-8
78. Vagenas NV, Kontoyannis CG, A methodology for quantitative determination of minor components in minerals based on FT-Raman spectroscopy: the case of calcite in dolomitic marble. *Vib Spectrosc.* 2003;32(2):261-264. doi:10.1016/S0924-2031(03)00027-4
79. Kristova P, Hopkinson L, Rutt K, Hunter H, Cressey G. Quantitative analyses of powdered multi-minerallic carbonate aggregates using a portable Raman spectrometer. *Am Min.* 2013;98(2-3):401-409. doi:10.2138/am.2013.4305
80. Veneranda M, Lopez-Reyes G, Pascual Sanchez E, et al. ExoMars Raman laser spectrometer: a tool to semiquantify the serpentinization degree of olivine-rich rocks on Mars. *Astrobiology*. 2021;21(3):307-322. doi:10.1089/ast.2020.2265
81. Carter J, Quantin C, Thollot P, Loizeau D, Ody A, Lozach L. Oxia planum, a clay-laden landing site proposed for the Exomars Rover mission: aqueous mineralogy and alteration scenarios. in 47th Lunar and Planetary Science Conference 2064 2016.
82. Quantin C, Carter J, Thollot P, Broyer J, Lozach L, Davis J, Grindrod P, Pajola M, Baratti E, Rossato S, Allemand P. Oxia Planum, the landing site for Exomars 2018. 47th Lunar Planet. Sci Conf 2863 2016.
83. Martin JD. Using XPowder: a software package for powder X-ray diffraction analysis. 2004.
84. Veneranda M, Manrique-Martinez JA, Garcia-Prieto C, et al. Raman semi-quantification on Mars: ExoMars RLS system as a tool to better comprehend the geological evolution of Martian crust. *Icarus*. 2021;367:114542. doi:10.1016/j.icarus.2021.114542
85. Demaret L, Hutchinson IB, Eppe G, Malherbe C. Quantitative analysis of binary and ternary organo-mineral solid dispersions by Raman spectroscopy for robotic planetary exploration missions on Mars. *Analyst*. 2022;146(23):7306-7319. doi:10.1039/d1an01514a
86. Wiens RC, Maurice S, Perez FR. The SuperCam remote sensing instrument suite for the mars 2020 rover: a preview. *Spectrosc*. 2017;32:50-55.
87. Gasda PJ, Anderson RB, Cousin A, et al. Quantification of manganese for ChemCam Mars and laboratory spectra using a multivariate model. *Spectrochim Acta Part B at Spectrosc*. 2021;181:106223. doi:10.1016/j.sab.2021.106223
88. Wiens RC, Maurice S, Lasue J, et al. Pre- flight calibration and initial data processing for the ChemCam laser-induced breakdown spectroscopy instrument on the Mars Science Laboratory rover. *Spectrochim Acta Part B*. 2013;82:1-27. doi:10.1016/j.sab.2013.02.003
89. Clegg SM, Wiens RC, Anderson R, et al. Recalibration of the Mars Science Laboratory ChemCam instrument with an expanded geochemical database. *Spectrochim Acta - Part B at Spectrosc*. 2017;129:64-85. doi:10.1016/j.sab.2016.12.003
90. Fabre C, Cousin A, Wiens RC, et al. Spectrochimica Acta Part B in situ calibration using univariate analyses based on the onboard ChemCam targets: first prediction of Martian rock and soil compositions. *Spectrochim Acta Part B at Spectrosc*. 2014;99:34-51. doi:10.1016/j.sab.2014.03.014
91. Payré V, Fabre C, Cousin A, et al. Alkali trace elements in Gale crater, Mars, with ChemCam: calibration update and geological implications. *J Geophys Res Planets*. 2017;122(3):650-679. doi:10.1002/2016JE005201
92. Anderson RB, Forni O, Cousin A, et al. Post-landing major element quantification using SuperCam laser induced breakdown spectroscopy. *Spectrochim Acta Part B: At Spectrosc*. 2022;188:106347.
93. Moros J, Laserna J. New Raman—laser-induced breakdown spectroscopy identity of explosives using parametric data fusion on an integrated sensing platform. *Anal Chem*. 2011;83(16):6275-6285. doi:10.1021/ac2009433
94. Moros J, Laserna JJ. Unveiling the identity of distant targets through advanced Raman-laser-induced breakdown spectroscopy data fusion strategies. *Talanta*. 2015;134:627-639. doi:10.1016/j.talanta.2014.12.001
95. Prochazka D, Mazura M, Samek O, et al. Combination of laser-induced breakdown spectroscopy and Raman spectroscopy for multivariate classification of bacteria. *Spectrochimica Acta Part B*. 2018;139:6-12. doi:10.1016/j.sab.2017.11.004
96. Zhao M, Markiewicz-Keszycka M, Beattie RJ, et al. Quantification of calcium in infant formula using laser-induced breakdown spectroscopy (LIBS), Fourier transform mid-infrared (FT-IR) and Raman spectroscopy combined with chemometrics including data fusion. *Food Chem*. 2020;320:126639. doi:10.1016/j.foodchem.2020.126639

97. Manrique-Martinez JA, Lopez-Reyes G, Alvarez-Perez A, et al. Evaluation of multivariate analyses and data fusion between Raman and laser-induced breakdown spectroscopy in binary mixtures and its potential for solar system exploration. *J Raman Spectrosc*. 2020;1–16 (9):1702-1717. doi:10.1002/jrs.5819
98. Gibbons E, Léveillé R, Berlo K. Spectrochimica Acta Part B data fusion of laser-induced breakdown and Raman spectroscopies: enhancing clay mineral identification. *Spectrochim Acta Part B*. 2020;170:105905. doi:10.1016/j.sab.2020.105905
99. Moros J, Elfaham MM, Laserna JJ. Dual-spectroscopy platform for the surveillance of Mars mineralogy using a decisions fusion architecture on simultaneous LIBS-Raman data. *Anal Chem*. 2018;90(3):2079-2087. doi:10.1021/acs.analchem.7b04124

How to cite this article: Veneranda M, Manrique JA, Sanz-Arranz A, et al. Application of chemometrics on Raman spectra from Mars: Recent advances and future perspectives. *Journal of Chemometrics*. 2022;e3438. doi:10.1002/cem.3438